BMB
reports

Intrinsic bent DNA colocalizes with the sequence involved in the *Nd-s*^{D} mutation in the *Bombyx mori* fibroin light chain gene

Joice Felipes Barbosa[1], *Juliana Pereira Bravo*[1], *Karen Izumi Takeda*[1], *Daniela Bertolini Zanatta*[1], *José Luis da Conceição Silva*[1], *Valério Américo Balani*[1], *Adriana Fiorini*[2] *& Maria Aparecida Fernandez*[1,*]

[1]Departamento de Biologia Celular e Genética, Universidade Estadual de Maringá - 87020-900, Maringá, Paraná, Brasil. [2]Centro Universitário de Maringá, CESUMAR - 87050-390, Maringá, Paraná, Brasil.

Multiple sequence alignments of the *Bombyx mori* fibroin light chain gene (*fib-L*) from hybrids and from Chinese and Japanese strains demonstrated that 51.6% of the *fib-L* third intron is conserved. One of these conserved segments, 41 bp long, contains the sequence CGTTATTATACATATT, which is duplicated in the *B. mori Nd-s*^{D} mutant. In the present work, electrophoretic mobility assays and computational analyses revealed a major peak of intrinsic bent DNA within the segment that undergoes breakage in the previously-described *Nd-s*^{D} mutation. This result suggested that this intrinsically-curved region might mediate DNA cleavage and enhance recombination events in the third intron of the *Bombyx mori fib-L* gene. [BMB reports 2008; 41(5): 394-399]

INTRODUCTION

Bombyx mori, the mulberry silkworm, is a model organism for *Lepidoptera*, the second most numerous insect order and one that contains many species important for agriculture and forestry. *B. mori* has been domesticated for silk production for 5,000 years (1) and provides the major source of income for 30 million families in China, India, Vietnam, Thailand, and Brazil. Advances in silkworm research have significantly improved sericulture and facilitated the development of new pest control strategies. In addition, with the development of biotechnology, *B. mori* has emerged as an important bioreactor for the production of recombinant proteins (2-4).

The silk moth domestication process has established more than 3,000 strains of *B. mori*. Besides the many different geographical and ancestral races, there are inbred and mutant lines that carry numerous genetic variants, some of which directly relate to the quality and yield of silk (5). Generally speaking, *B. mori* strains of temperate geographic origin are good silk producers, while the tropical ones produce lower silk quantities but are more resistant to disease and adverse climatic conditions. Differences in silk production among *B. mori* strains have prompted studies of the genetic factors involved in the yield and quality of silk (5).

Silk fibroin is secreted into the lumen of the posterior silk gland (PSG) of the *B. mori* silkworm and is mainly composed of three polypeptides: a 350-kDa heavy chain (H-chain; 6), a 26-kDa light chain (L-chain; 7), and fibrohexamerin (fhx; 8). The fibroin light chain gene (*fib-L*) maps to chromosome 14, is 14,626 base pairs (bp) long, and contains seven exons with large introns (9). The first intron occupies about 60% of the gene, and the other introns together account for approximately 31% (9); therefore, 91% of the gene is composed of non-coding DNA.

The *Nd-s* and *Nd-s*^{D} mutations are found in the third intron of the *fib-L* gene and result in a downstream deletion of exon III and enhanced aberrant recombination with downstream sequences (10). The *Nd-s* mutant was initially identified in 1960 in one specific strain of *B. mori*, and the *Nd-s*^{D} mutant was identified four generations after injecting diethyl sulphate into a male pupa from a normal *B. mori* of unknown strain (11). These mutants have immature PSGs and secrete less than 1% of the normal level of fibroin, which leads to the production of a very thin, naked-pupa cocoon that consists mostly of sericin (10).

Detailed analysis of several known recombination sites has demonstrated that they are located at the bottom regions of DNA loops (12-14). Mutations, breakpoints, and recombination events are commonly associated with bent DNA, and they may preferentially occur at DNA loop anchorage sites, which could lead to deletion or repositioning of individual DNA loops (15). Intrinsic bends in the DNA sequence occur in 2- to 6-bp adenine-thymine tracts (A/T) at intervals of approximately 10 bp (or multiples of 10) (16). Bent DNA sites are involved in biological processes such as DNA recombination (15, 17), fragile sites (18), replication (19, 20), transcription (21-23), nucleosome formation (24), and scaffold/matrix attachment regions (S/MARs) (25).

This work described the physical structure of the *fib-L* gene and verified the presence of intrinsic bent DNA in the third intron, using electrophoretic mobility assays and 2D structures

*Corresponding author. Tel: 55-44-3261-4700; Fax: 55-44-3261-4893; E-mail: aparecidafernandez@gmail.com

Received 4 February 2008, Accepted 10 March 2008

Keywords: *Bombyx mori*, *fib-L* third intron, Fibroin light chain gene, Intrinsic bent DNA sites, *Nd-s*^{D} mutation

of the 3D projection. The results showed that the main peak of intrinsic curvature lies within the *fib-L* gene segment containing the previously-described *Nd-s*^{D} mutation. Therefore, we propose that this mutation could be related to the bent DNA site in the *fib-L* third intron.

RESULTS AND DISCUSSION

Electrophoretic mobility assay

Our research team previously conducted multiple alignments with *Bombyx mori fib-L* third intron sequences from hybrids and from Chinese and Japanese strains (Fig. 1; supplementary material 1 and 2; 26). These sequence alignments demonstrated that 51.6% of the sequence of this intron contains conserved regions, one of which is a 41-bp segment containing the CGTTAT TATACATATT sequence (positions 10973 to 10988; Fig. 1) that is duplicated in the *Nd-s*^{D} mutant.

Since DNA fragments containing unusual structures generally show an anomalous mobility during polyacrylamide gel electrophoresis (25), electrophoretic mobility assays are a powerful tool to investigate the curvature of DNA segments. To analyze whether the structure of the *fib-L* third intron was curved, we cloned 903-bp amplified gene products from the Chinese C121A and C122B *B. mori* strains into the PCR® 2.1-TOPO® plasmid (Invitrogen). We then analyzed their migration patterns in agarose (AGA), polyacrylamide (PA), and polyacrylamide with ethidium bromide (PA + EtBr) gels. AGA forms an irregular mesh upon polymerization, and migration of DNA fragments in AGA gels depends solely on the fragment size. In PA gels, however, migration depends on both fragment size and structure. Differences between migration patterns in AGA and PA gels suggest curvature in the DNA of interest. In the PA + EtBr gels, ethidium bromide intercalates into the DNA molecule and opens up its structure, abolishing any altered PA migration. Therefore, a reversion of the PA migration pattern in the PA + EtBr gels confirms the presence of curvature in the DNA. The fragment mobility reduction, or R-value, is the ratio between the observed size in each gel system and the real fragment size. R-values ≥ 1.11 indicate reduced mobility, indicative of bent DNA (27).

The fragments from the C121A and C122B clones showed normal migration in AGA and PA + EtBr gels but a strong migration reduction in PA gels (Fig. 2, gray arrow). Comparing the migrations revealed PA-associated R-values of 1.64 for C121A and 1.59 for C122B, indicating that the *fib-L* third intron has a curved structure. The linearized PCR®2.1-TOPO® plasmid, our positive control for bent DNA, showed a fast migration in the PA gel (Fig. 2, black arrow), because this plasmid has a strong peak of curvature in the 5′ end. Fragments with faster mobility are characteristic of fragments with bent regions in one or both fragment ends (25). The plasmid pBluescript II (cleaved with *Bam*HI restriction enzyme), which does not display mobility alterations with this technique, was included as a negative control (Fig. 2, dark gray arrow).

In silico analysis

To further characterize the structure of the *fib-L* gene third intron, we subjected the corresponding ~680 bp fragments from the C121A and C122B strains to theoretical 2D modeling and calculated the parameter helical ENDS ratio, a measure of DNA curvature in the 2D model. Fig. 3 shows the 2D projection of the 3D path and the ENDS ratio of the C121A (A) and C122B (B) *fib-L* third intron DNA fragments. Interestingly, the two sequences showed a stronger ENDS ratio value (1.5) in the region of the *fib-L* gene containing the previously-described *Nd-s*^{D} mutation. The observed peak localized to the center of the most curved point in the structure (Fig. 3, small circle), regardless of variations in the angles (30 and 60 degrees) in the secondary structure (Fig. 3A and B, respectively). This result suggested that the intrinsic DNA bending site in this segment was important for fragment shape maintenance.

Fig. 4 shows the analysis of the 200 nucleotides surrounding the bent DNA site (rectangle) in the C121A and C122B third intron *fib-L* gene. This sequence analysis revealed dA.dT tract distribution in 10-bp intervals or multiples thereof (bold), characteristic of curved DNA. There are four CAnT motifs

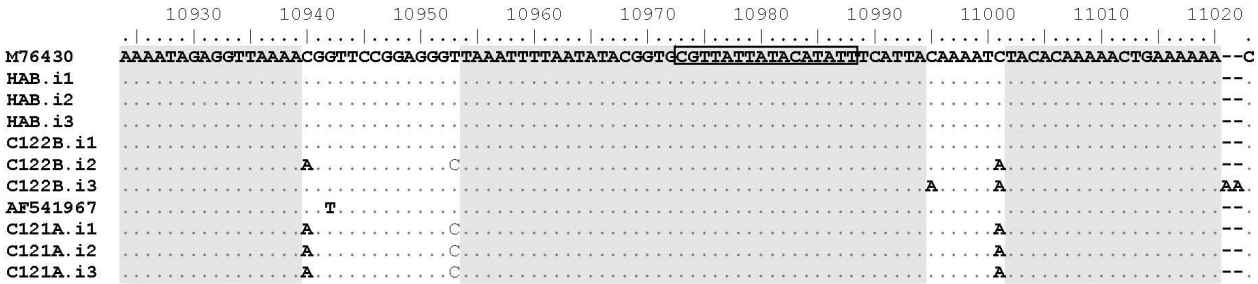

Fig. 1. Alignment of partial sequences of *fib-L* third intron genes from different *B. mori* strains. DNA sequence sources and geographical origins are provided in Supplementary Material 2. In this alignment, the Japanese strain M76430 was used as a reference. The dots represent homology to the M76430 sequence. Dashes indicate insertion/ deletion events. Nucleotide transitions and transversions are shown in bold, and the gray regions delimit the conserved regions. The sequence that is duplicated in *Nd-s*^{D} mutation is boxed. A complete alignment of the *fib-L* third intron gene is shown in the Supplementary Material 1.

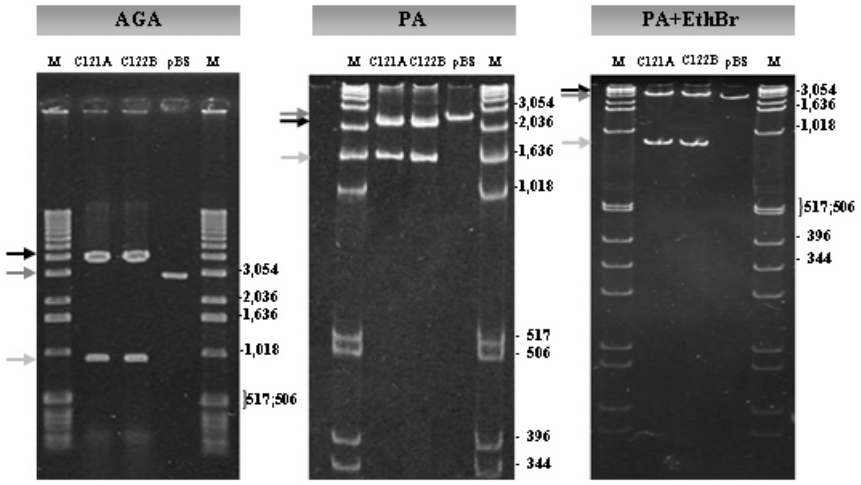

Fig. 2. Electrophoretic mobility assay of the ~900 bp *fib-L* third intron gene restriction fragments from C121A and C122B clones, utilizing 1.0% agarose gels (AGA) or 6% polyacrylamide gels without (PA) and with (PA + EtBr) ethidium bromide. Both fragments (gray arrow) showed reduced mobility in PA, with R-values of 1.64 for C121A and 1.59 for C122B. The black arrow indicates the PCR®2.1-TOPO® plasmid (positive control) and the dark gray arrow the linearized pBluescript II plasmid (pBS; negative control). M, 1kb molecular weight marker (Invitrogen).

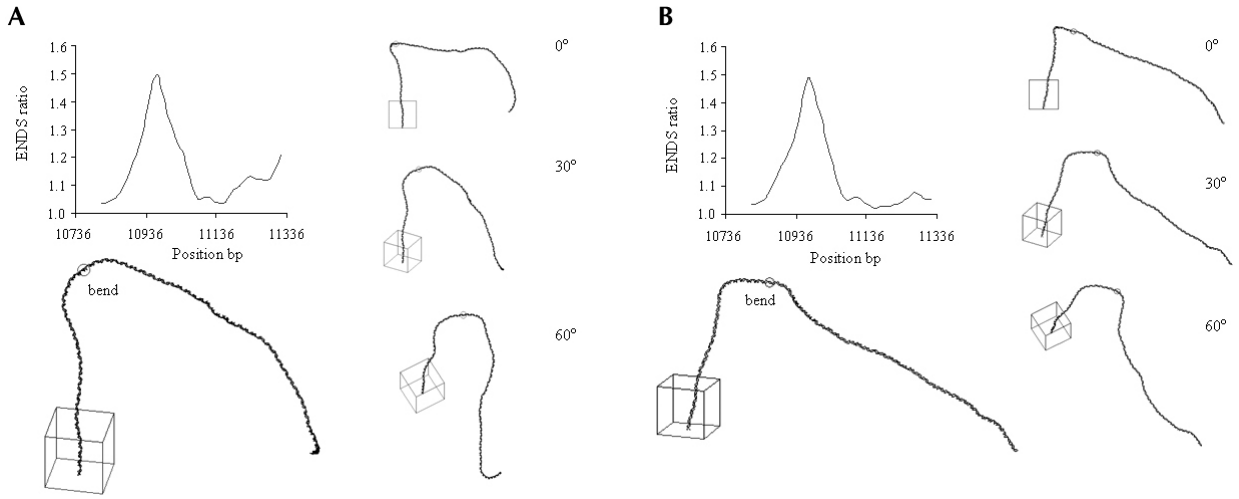

Fig. 3. ENDS ratio and 2D projection of 3D DNA path of the C121A (A) and C122B (B) *fib-L* third intron gene sequences. The two sequences showed stronger curvature, with an ENDS ratio of 1.50. Rotation of these fragments by 30 and 60 degrees confirmed that the bent regions (small circles) are important for maintaining the fragment shape.

(double underlined) in the C121A sequence and three in the C122B. This motif yields a stronger curvature, because the adenine tracts flanked by cytosine on the 5′ end and thymidine on the 3′ end induce local bends, which together produce a stronger global bend (22).

Intrinsic DNA curvature reportedly facilitates the binding of proteins such as DNA topoisomerase I and II (25). In principle, bent DNA might also facilitate the binding of diethyl sulphate or other compounds, such as insecticides, that are used in agriculture. Such compounds could produce breaks and recombination events, thereby inducing gene mutation.

Our results raise new questions about the structure of the *fib-L* third intron. Can this bent structure increase the likelihood of recombination in this chromosomal segment? Is it possible that in the *Nd-s*^{D} mutation, the described 16-bp sequence nucleotide duplicates before the segment break? If so, is this duplication the reason for the breakage? Although previous reports suggested that the *Nd-s* mutant was achieved through population breeding and the *Nd-s*^{D} was obtained from diethyl sulphate treatment, they did not find an additional 16-bp sequence in the downstream region of the chromosome (10), where the breakage and joint point for the new mutated sequence occurs. However, diethyl sulphate and related carcinogenic compounds might be able to duplicate segments and break the DNA molecule; and the intrinsic bent curvature of the DNA might enhance that ability, as reported elsewhere (17). Addressing these issues will require a search for the 16-bp sequence duplication prior to the third intron breakage event using *B. mori* strains that

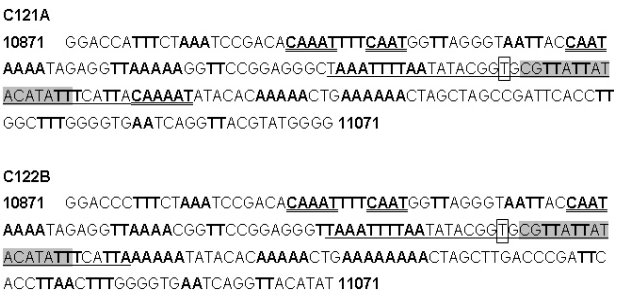

Fig. 4. Sequence analysis of the bent DNA sites in the C121A and C122B *fib-L* third intron gene. The 200-bp nucleotide sequences surrounding the nucleotide in the center (rectangle) of the bent DNA sites were analyzed. The dA.dT tracts with two or more nucleotides are shown in bold, the CAnT motif is double underlined, the CGTTATTATACATATT sequence is shadowed, and the 41-bp conserved sequence is underlined.

are heterozygous for the *fib-L* gene and/or breeds treated with alkylating agents. Functional experiments with transgenic silkworm lines in which the intrinsic bent structure of this intron is abolished by point mutations could also be helpful in answering such questions. Understanding more about the mechanisms involved in chromosomal recombination will expand our knowledge in this area, and these mechanisms may represent a powerful tool to further the understanding of mutation processes in eukaryotic cells.

MATERIALS AND METHODS

Bombyx mori strains

B. mori strains were provided by COCAMAR (Cooperativa Agroindustrial; Maringá, Parana State, Brazil) to the Universidade *Estadual de Maringá*, Parana State, Brazil. Silkworms were raised at 25°C with fresh mulberry leaves at a COCAMAR farm.

DNA extraction

Genomic DNA was extracted from the silk glands of five-day-old fifth instar larvae using a modification of a previously-described protocol (28). Briefly, pairs of silk glands were dissected and incubated in 3 ml of extraction buffer (1.5% sarkosil, 50 mM EDTA [pH 8], 10 mM NaCl, and 1 mg/ml proteinase K) for 2-3 hours at 50°C. The extract was subjected to one round of chloroform (chloroform/isoamylalcohol 24:1) and three rounds of phenol (pH 8.0), ethanol precipitated with 0.2 M NaCl and 0.7 volume of isopropanol, and resuspended in TE buffer (10 mM Tris-HCL [pH 8.0] and 1 mM EDTA [pH 8.0]). DNA concentration was determined by spectrophotometry.

PCR and cloning

PCR primers for the amplification of the third intron of *fib-L* were constructed using FAST-PCR software (version 3.5.30 by Ruslan Kalendar). The forward primer sequence (5′-ACGTCGA TGGGACTACGTCG-3′) and reverse primer sequence (5′-CGG ACCTGACGCCGTCTGTG-3′) are complementary to the third and fourth exons, respectively. PCR was performed routinely, in a final volume of 15 µl: 2.5 mM dNTPs, 100 ng of DNA, 25 pmol of each primer, 1X PCR buffer (with 1.5 mM of $MgCl_2$), and 1 unit of Taq Polymerase (Invitrogen). The amplification conditions were 1 min at 94°C, 1 min at 58°C, and 1 min at 72°C, for a total of 35 cycles, followed by a final extension of 10 min at 72°C. PCR products were purified using a PCR purification Kit (Qiagen) and cloned using a TOPO TA PCR Cloning Kit (Invitrogen). The PCR products, approximately 900 bp long, were cloned from one individual of the strain C121A and one individual of the strain C122B, and subsequent analyses were carried out with these PCR products.

Sequencing

Sequencing reactions were performed with the DYEnamic ET Dye Terminator Kit (Amersham Biosciences), and the reactions products were analyzed with a MegaBACE 1000 automated DNA sequencer (Amersham Biosciences).

Electrophoresis mobility assay and computational analysis

Fragments from recombinant pC121A and pC122B clones were obtained by digestion with the *Eco*RI restriction enzyme. The mobility of the fragments was compared under the following conditions: electrophoresis in 1% agarose gels (control gels) at 3.5 Volts/cm at room temperature, and electrophoresis in 6% polyacrylamide gels (acrylamide/bisacrylamide ratio 30:0.8) at 7 Volts/cm at 4°C, for 12 hours. To confirm the presence of bent DNA, the samples were incubated overnight in 1 µg/ml ethidium bromide (EthBr) and electrophoresed in 6% polyacrylamide gels that had been previously run with 1 µg/ml ethidium bromide in the running buffer. The ethidium bromide acts locally between base pairs, abolishing the intrinsic DNA curvature and straightening the fragments (25). All gels were run in 1X TBE buffer (45 mM Tris-borate, 1mM EDTA, pH 8.0), visualized with 0.1 µg/ml EthBr, and documented with a UVP BioImaging System under UV light. In all three gel systems, an *R*-value (corresponding to the ratio of the observed length to the expected length) was calculated for each DNA fragment to determine the mobility alteration in the gels.

The nucleotide sequences for C121A and C122B (GenBank accession numbers EF050754 and EF050757, respectively) were analyzed by computational modelling using the Trifonov dinucleotide wedge model for curvature study. The projection of the three dimensional path and helical parameters were obtained with Map15a and 3D15m1 software using the algorithm of Eckdahl and Anderson (29) and the helical parameters of Bolshoy *et al.* (30), as previously described (31, 32).

Putative intrinsic bent DNA sites identified by the ENDS ratio (ratio of the contour length of the segments' helical axis to the shortest distance between the fragments' ends) were computed at a window of 150 bp width and a 10 bp step.

Acknowledgements
We thank Valmir Peron and Marli Licero Schuete Silva for their dedicated technical assistance. JF receive a graduate fellowship from CNPq, and JPB and DBZ receive fellowships from CAPES. This work was supported by grants from CNPq, FINEP, Fundação Araucária, Secretaria de Estado da Ciência, Tecnologia e Ensino Superior, SETI, FUNDO PARANA, The Academy of Sciences for Developing World-TWAS and Science and Innovation Santander Banespa 2006 Prize.

REFERENCES

1. Xiang, Z. H. (1995) In Genetics and Breeding of the Silkworm, *Chinese Agriculture Press, Beijing*, pp. 273-289.
2. Tamura, T., Thibert C, Royer, C., Kanda, T., Abraham, E., Kamba, M., Komoto, N., Thomas, J. L., Mauchamp, B., Chavancy, G., Shirk, P., Fraser, M., Prudhomme, J. C. and Couble, P. (2000) Germline transformation of the silkworm *Bombyx mori* L. using a piggyBac transposon-derived vector. *Nat. Biotechnol.* **18**, 81-84.
3. Tomita, M., Munetsuna, H., Sato, T., Adachi, T., Hino, R., Hayashi, M., Shimizu, K., Nakamura, N., Tamura, T. and Yoshizato, K. (2003) Transgenic silkworms produce recombinant human type III procollagen in cocoons. *Nat. Biotechnol.* **21**, 52-56.
4. Royer, C., Jalabert, A., da Rocha, M., Grenier, A. M., Mauchamp, B., Couble, P. and Chavancy, G. (2005) Biosynthesis and cocoon-export of a recombinant globular protein in transgenic silkworms. *Transg. Res.* **14**, 463-472.
5. Nagaraju, J. (2000) Recent advances in molecular genetics of the silk moth, *Bombyx mori*. *Current Sci.* **78**, 151-161.
6. Shimura, K.(1983) Chemical composition and biosynthesis of silk proteins. *Experimentia* **39**, 455-461.
7. Yamaguchi, K., Kikuchi, Y., Takagi, T., Kikuchi, A., Oyama, F., Shimura, K. and Mizuno, S. (1989) Primary structure of the silk fibroin light chain determined by cDNA sequencing and peptide analysis. *J. Mol. Biol.* **210**, 127-139.
8. Inoue, S., Tanaka, K., Arisaka, F., Kimura, S., Ohtomo, K. and Mizuno, S. (2000) Silk fibroin of *Bombyx mori* is secreted, assembling a high molecular mass elementary unit consisting of H-chain, L-chain, and P25, with a 6:6:1 molar ratio. *J. Biol. Chem.* **275**, 40517-40528.
9. Kikuchi, Y., Mori, K., Suzuki, S., Yamaguchi, K. and Mizuno, S. (1992) Structure of the *Bombyx mori* fibroin light-chain-encoding gene: upstream sequence elements common to the light and heavy chain. *Gene* **110**, 151-158.
10. Mori, K., Tanaka, K., Kikuchi, Y., Waga, M., Waga, S. and Mizuno, S. (1995) Production of a chimeric fibroin light-chain polypeptide in a fibroin secretion-deficient naked pupa mutant of the silkworm *Bombyx mori*. *J. Mol. Biol.* **251**, 217-228.
11. Gamo, T. and Sato, S. (1985) Ultrastructural study of the posterior silk gland in the *Nd*, *Nd-s^D* mutants with a defect of fibroin synthesis. *J. Seric. Sci. Jpn.* **54**, 412-419.
12. Razin, S. V. (1999) Chromosomal DNA loops may constitute basic units of the eukaryotic genome organization and evolution. *Crit. Rev. Eukaryot. Gene Expr.* **9**, 279-283.
13. Bode, J., Benham, C., Ernst, E., Knopp, A., Marschalek, R., Strick, R. and Strissel, P. (2000) Fatal connections: when DNA ends meet on the nuclear matrix. *J. Cell. Biochem.* **35**, 3-22.
14. Svetlova, E. Y., Razin, S. V., Debatisse, M. (2001) Mammalian recombination hot spot in a DNA loop anchorage region: A model for the study of common fragile sites. *J. Cell. Biochem.* **81**, 170-178.
15. Iarovaia, O. V., Bystritskiy, A., Ravcheev, D., Hancock, R. and Razin, S. V. (2004) Visualization of individual DNA loops and a map of loop domains in the human dystrophin gene. *Nucleic Acids Res.* **32**, 2079-2086.
16. Calladine, C. R., Drew, H. R., Luisi, B. F., and Travers, A. A. (2004) Twisting and Curving. In "Understanding DNA: The molecule and how it works", eds. Academic Press, London, pp. 64-93.
17. Milot, E., Belmaaza, A., Wallenburg, J. C., Gusew, N., Bradley, W. E. and Chartrand, P. (1992) Chromosomal illegitimate recombination in mammalian cells is associated with intrinsically bent DNA elements. *EMBO J.* **13**, 5063-5070.
18. Palin, A. H., Critcher, R., Fitzgerald, D. J., Anderson, J. N., and Farr, C. J. (1998) Direct cloning and analysis of DNA sequences from a region of the Chinese hamster genome associated with aphidicolin-sensitive fragility. *J. Cell Sci.* **11**, 1623-1624.
19. Altman, A. L., and Fanning, E. (2004) Defined sequence modules and an architectural element cooperate to promote initiation at an ectopic mammalian chromosomal replication origin. *Mol. Cell. Biol.* **24**, 4138-4150.
20. Fiorini, A, Gouveia, F. de S., Soares, M. A. de M., Stocker, A. J., Ciferri, R. R. and Fernandez, M. A. (2006) DNA Bending in the Replication Zone of the C3 DNA Puff Amplicon of *Rhynchosciara americana* (Diptera: Sciaridae). *Mol. Biol. Rep.* **33**, 71-82.
21. Fiorini, A., Basso, L. R., Paçó-Larson, M. L. and Fernandez M. A. (2001) Mapping of intrinsic bent DNA sites in the upstream region of DNA puff *BhC4-1* amplified gene. *J. Cell. Biochem.* **83**, 1-13.
22. Ohyama, T. (2005) Curved DNA and transcription in eukaryotes. In "DNA conformation and transcription", ed. Springer Science + Business Media, New York, pp. 66-74.
23. Gouveia, F. de S., Gimenes F., Fiorini, A. and Fernandez, M. A. (2008) Intrinsic Bent DNA Sites in the Developmentally Amplified *C3-22* Gene Promoter of *Rhynchosciara americana* (Diptera: Sciaridae). *Biosci. Biotechnol. Biochem. in press*.
24. Virstedt, J., Berge, T., Henderson, R. M., Waring, M. J., and Travers, A. A. (2004) The influence of DNA stiffness uon nucleosome formation. *J. Struct. Biol.* **148**, 66-85.
25. Fiorini, A., Gouveia, F. de S. and Fernandez, M. A. (2006) Scaffold/Matrix Attachment Regions and intrinsic DNA curvature. *Biochemistry (Moscow)* **71**, 481-488.
26. Felipes, J., Bravo, J. P., Zanatta, D. B. and Fernandez, M. A. (2006) Sequence Variability in the Third Intron of *Bombyx mori* L-Chain (*fib-L*) Gene Amongst Different Strains. In: XXXV Annual Meeting of the Brazilian Society for Biochemistry and Molecular Biology (SBBq). Abstract ID:9020. http://sbbq.iq.usp.br/arquivos/2006/cdlivro/resumos/R9020.html

27. de Souza, O. N. and Ornstein, R. L. (1998) Inherent DNA curvature and flexibility correlate with TATA box functionality. *Biopolymers* **46**, 403-415.
28. Mills, D. R. and Goldsmith, M. R. (2000) Characterization of early follicular cDNA library suggests evidence for genetic polymorphisms in the inbred strain C108 of *Bombyx mori*. *Genes Genet. Syst*. **75**, 105-13.
29. Eckdahl, T. T.and Anderson, J. N. (1987) Computer modelling of DNA structures involved in chromosome maintenance. *Nucleic Acids Res*. **15**, 8531-8545.
30. Bolshoy, A., McNamara, P., Harrington, R. E. and Trifonov, E. N. (1991) Curved DNA without A-A: experimental estimation of all 16 DNA wedge angles. *Proc. Natl. Acad. Sci. U.S.A*. **88**, 2312-2316.
31. Pasero, P., Sjakste, N., Blettry, C., Got, C. and Marilley, M. (1993) Long-range organization and sequence-directed curvature of *Xenopus laevis* satellite 1 DNA. *Nucleic Acids Res*. **21**, 4703-4710.
32. Marilley, M. and Pasero, P. (1996) Common DNA structural features exhibited by eukaryotic ribosomal gene promoters. *Nucleic Acids Res*. **24**, 2204-2211.